Ataxin-1 regulates B cell function and the severity of autoimmune experimental encephalomyelitis

Alessandro Didonna[a,1], Ester Canto Puig[a], Qin Ma[a], Atsuko Matsunaga[a], Brenda Ho[a], Stacy J. Caillier[a], Hengameh Shams[a], Nicholas Lee[a], Stephen L. Hauser[a], Qiumin Tan (谭秋敏)[b], Scott S. Zamvil[a,c], and Jorge R. Oksenberg[a]

[a]Weill Institute for Neurosciences, Department of Neurology, University of California, San Francisco, CA 94158; [b]Department of Cell Biology, University of Alberta, Edmonton, AB T6G 2H7, Canada and [c]Program in Immunology, University of California, San Francisco, CA 94158

Edited by Lawrence Steinman, Stanford University School of Medicine, Stanford, CA, and approved August 5, 2020 (received for review February 28, 2020)

Ataxin-1 (ATXN1) is a ubiquitous polyglutamine protein expressed primarily in the nucleus where it binds chromatin and functions as a transcriptional repressor. Mutant forms of ataxin-1 containing expanded glutamine stretches cause the movement disorder spinocerebellar ataxia type 1 (SCA1) through a toxic gain-of-function mechanism in the cerebellum. Conversely, ATXN1 loss-of-function is implicated in cancer development and Alzheimer's disease (AD) pathogenesis. *ATXN1* was recently nominated as a susceptibility locus for multiple sclerosis (MS). Here, we show that *Atxn1*-null mice develop a more severe experimental autoimmune encephalomyelitis (EAE) course compared to wildtype mice. The aggravated phenotype is mediated by increased T helper type 1 (Th1) cell polarization, which in turn results from the dysregulation of B cell activity. Ataxin-1 ablation in B cells leads to aberrant expression of key costimulatory molecules involved in proinflammatory T cell differentiation, including cluster of differentiation (CD)44 and CD80. In addition, comprehensive phosphoflow cytometry and transcriptional profiling link the exaggerated proliferation of ataxin-1 deficient B cells to the activation of extracellular signal-regulated kinase (ERK) and signal transducer and activator of transcription (STAT) pathways. Lastly, selective deletion of the physiological binding partner capicua (CIC) demonstrates the importance of ATXN1 native interactions for correct B cell functioning. Altogether, we report a immunomodulatory role for ataxin-1 and provide a functional description of the *ATXN1* locus genetic association with MS risk.

multiple sclerosis | autoimmunity | antigen presentation | B cells | ataxin-1

The discovery of the *ATXN1* gene and the subsequent molecular characterization of its protein product ataxin-1 have taken place mostly in the context of spinocerebellar ataxia type 1 (SCA1) (1). Ataxin-1 contains an unstable polyglutamine (polyQ) domain, which can undergo pathological expansion and cause the selective neurodegeneration of cerebellar Purkinje cells—the principal site of SCA1 pathology—resulting in progressive motor incoordination. Mutant ataxin-1 escapes the standard cellular systems of protein degradation and accumulates within the nuclear compartment of neuronal cells, where it exerts its pathogenic activity through a toxic gain-of-function mechanism (2). Ataxin-1 is able to bind chromatin and interacts with a number of known transcriptional repressors, indicating a role in the regulation of gene expression (3). However, the full spectrum of ataxin-1 functions is far from being fully described.

Mice lacking ataxin-1 are viable, fertile, and do not show any evidence of ataxia or neurodegeneration. Notwithstanding the lack of gross phenotypes, *Atxn1*-null mice display decreased exploratory behavior and impaired performance on the rotarod apparatus and water maze test (4). A body of experimental evidence also supports a role for ataxin-1 in neurodevelopment, adult neurogenesis, and extracellular matrix remodeling (5–7). In addition, ataxin-1 controls cell proliferation and the epithelial-mesenchymal transition (EMT) of cancer cells (8). More recently, ataxin-1 loss-of-function was shown to elevate beta secretase 1 (BACE1) expression and aggravate Aβ pathology, proposing ataxin-1 as a potential contributor to Alzheimer's disease (AD) risk (9).

Multiple sclerosis (MS) is a chronic disorder of the central nervous system (CNS) characterized by focal lymphocyte infiltration, breakdown of myelin sheaths, proliferation of astrocytes, and axonal degeneration. Although the primary etiology remains unknown, the interplay between genetic and environmental factors is believed to initiate MS pathogenesis (10). In a recent large-scale genomic effort, the locus containing the *ATXN1* gene was found associated with MS susceptibility (11). Here, we build on this discovery to characterize the role of ataxin-1 in the context of CNS autoimmunity. By employing the MS model experimental autoimmune encephalomyelitis (EAE) in *Atxn1*-null mice, we show that ataxin-1 exerts a B cell-mediated protective effect on autoimmune demyelination, enabled by native interactions with the transcriptional repressor capicua (CIC).

Results

Ataxin-1 Exerts a Protective Activity on Autoimmune Demyelination. The known genetic contributions to MS risk consist of 232 autosomal risk variants (11). This map includes a region in chromosome 6p22.3 (position 16672769 in hg19), in which the marker rs719316 in the third intron of the *ATXN1* gene represents the strongest association ($P = 1.62 \times 10^{-13}$, odds ratio (OR) = 1.072)

Significance

Over 200 genomic loci have been found associated with the risk of developing multiple sclerosis (MS). Despite this important body of data, limited information exists on the cellular pathways and molecular mechanisms underlying MS genetic complexity. In this study, we report the functional characterization of the ataxin-1 encoding *ATXN1* susceptibility locus. Ataxin-1 is a polyglutamine protein that is classically associated with the neurodegenerative disorder spinocerebellar ataxia type 1 (SCA1). Here, we show that ataxin-1 also exerts a protective activity against autoimmune demyelination in a preclinical model of MS. This function is associated with an immunomodulatory role mainly targeting the B cell compartment. Altogether, these findings expand our current knowledge on both MS pathogenesis and ataxin-1 biology.

Author contributions: A.D., S.L.H., S.S.Z., and J.R.O. designed research; A.D., E.C.P., Q.M., A.M., B.H., S.J.C., N.L., and Q.T. performed research; Q.T. contributed new reagents/analytic tools; A.D., E.C.P., Q.M., H.S., S.S.Z., and J.R.O. analyzed data; and A.D., S.L.H., Q.T., S.S.Z., and J.R.O. wrote the paper.

The authors declare no competing interest.

This article is a PNAS Direct Submission.

[1]To whom correspondence may be addressed. Email: alessandro.didonna@ucsf.edu.

This article contains supporting information online at https://www.pnas.org/lookup/suppl/doi:10.1073/pnas.2003798117/-/DCSupplemental.

First published September 2, 2020.

in both fixed- and random-effects models (Fig. 1*A*). Subsequent analysis in African Americans possibly refined the association, with the top single nucleotide polymorphism (SNP) rs932411 mapping within the seventh intron of *ATXN1* ($P = 0.0022$) (12).

However, seven genes map to the *ATXN1* locus, each one representing a potential candidate that could explain the association with MS susceptibility. To discern among them, we applied a recently developed in silico approach, computing the regulatory potential of rs719316 to all of the neighboring genes in the extended haplotype block in the context of cell-specific protein networks (13). *ATXN1* showed the highest scores in all of the cell types analyzed (Fig. 1*B*), adding support to consider *ATXN1* as the most plausible disease risk gene within the locus. Concurrently, expression quantitative trait locus (eQTL) analysis in both brain and immune tissues [Genotype-Tissue Expression (GTEx) Portal] excluded long-range effects targeting genes outside the locus. Therefore, we decided to functionally validate this prediction in vivo exploring the role of *ATXN1* in EAE, a murine disease that recapitulates several clinical, immunological, and histopathological features of MS (14).

We generated *Atxn1* knockout ($Atxn1^{-/-}$), heterozygous ($Atxn1^{+/-}$), and wildtype ($Atxn1^{+/+}$) mice on a pure C57BL/6J background (*SI Appendix*, Fig. S1*A*), and we immunized 8 to 10 wk female mice of each genotype with myelin oligodendrocyte glycoprotein (MOG) peptide 35 to 55 ($MOG_{35–55}$). *Atxn1* knockout mice exhibited significant greater disease severity and higher mortality rates as compared to wildtype littermates (Fig. 1 *C* and *D*). Heterozygous animals showed a disease profile intermediate between the knockout and wildtype mice, suggesting an *Atxn1* gene dosage effect on EAE progression. Ataxin-1 deficiency did not affect disease onset. We then tested whether the protective function of ataxin-1 was dependent upon its polyglutamine domain. No significant differences were found in the disease course of knock-in animals bearing an *Atxn1* gene containing 154 cytosine-adenine-guanine (CAG) repeats ($Atxn1^{154Q/2Q}$) and wildtype controls ($Atxn1^{2Q/2Q}$) (*SI Appendix*, Fig. S1*B*), except for a short time window (22 to 23 dpi) (Fig. 1 *E* and *F*). Interestingly, the EAE profile of knock-in mice resembles EAE in $Atxn1^{+/-}$ animals. As expanded ataxin-1 forms insoluble aggregates within the nucleus, $Atxn1^{154Q/2Q}$ mice may function as partial knockout models for ataxin-1 physiological activity.

Ataxin-1 Regulates Th1 Differentiation. Ataxin-1 is expressed ubiquitously (15). Consequently, the exacerbated EAE course in constitutive knockout animals may be the result of ataxin-1 deficiency in multiple cells and tissues. In wildtype mice, the levels of *Atxn1* transcript and those of a splicing isoform are upregulated in splenocytes at the EAE peak (Fig. 2*A*), pointing out at a possible regulatory function of ataxin-1 in the immune system. To specifically address this hypothesis, we carried out adoptive transfer experiments in which splenocytes from MOG peptide-primed knockout animals were injected into wildtype recipients. Consistent with the active EAE experiments, mice that received $Atxn1^{-/-}$ cells developed more severe clinical and histopathological EAE phenotypes as compared to control animals injected with wildtype cells (Fig. 2*B* and *SI Appendix*, Fig. S2 *A* and *B*), confirming that ataxin-1 ablation in the immune system is sufficient per se to drive the aggravated disease. In agreement, a higher percentage of T helper type 1 (Th1) cells was measured in knockout splenocytes. In contrast, there were no significant changes in the frequencies of Th17 and regulatory T cells (Treg) populations between the two genotypes (Fig. 2*C*).

Considering the heterogeneity of splenocyte cultures, the increased Th1 polarization could reflect an intrinsic property of knockout cluster of differentiation $(CD)4^+$ T cells or, alternatively, an indirect mechanism where ataxin-1 loss in antigen-presenting cells (APCs) influences T cell differentiation. To discern between these two scenarios, we measured the propensity of isolated naïve $CD4^+$ T cells to differentiate toward Th1, Th17, and Treg lineages in response to nonselective T cell receptor stimulation via anti-CD3/anti-CD28 engagement. Under these conditions, no differences were detected between naïve knockout and wildtype T cells (Fig. 2*D*), suggesting that the elevated Th1 differentiation post-immunization and exacerbated phenotype of the $Atxn1^{-/-}$ strain could result from an indirect effect on APC function. To test this hypothesis, we analyzed by flow cytometry the cell surface expression of CD44 and CD80 in splenic T cells ($CD4^+$ and $CD8^+$), B cells, and monocytes. Both proteins are critical costimulatory molecules in T cell activation and promote Th1 differentiation (16, 17). Basal expression of both markers in naïve mice was increased in knockout B cells while CD44 was decreased in knockout T cells (Fig. 2*E* and *SI Appendix*, Table S1). A similar increase in CD44 and CD80 levels was also measured in knockout B cells and monocytes upon MOG peptide stimulation (Fig. 2*F* and *SI Appendix*, Table S1). B cells participate in Th1 reactivation in the nervous system (18, 19), and when used in vitro, B cells from $Atxn1^{-/-}$ mice were able to induce maximal T cell proliferation in $CD4^+$ lymphocytes from MOG-2D2 mice at lower concentrations of MOG peptide as compared to wildtype B cells (Fig. 2*G*), confirming that ataxin-1 ablation compromised their immunoregulatory function.

B Cells Are the Primary Target of Ataxin-1 in the Immune System. In order to fully capture the contribution of B cells to the EAE phenotype and precisely dissect the function of ataxin-1 in their biology, we characterized B cell populations in $Atxn1^{-/-}$ mice. First, we performed a thorough immunophenotyping of the different B cell subsets present in the spleens of naïve and MOG peptide immunized mice (20). In both conditions, we detected a significant increase of B-1a and B-1b cells in knockout animals as compared to controls, while marginal zone (MZ) B-2 cells were slightly, yet significantly decreased (Fig. 3*A* and *SI Appendix*, Fig. S3). No differences were measured in the frequency of follicular B-2 and regulatory B cells between the two genotypes (Fig. 3*A* and *SI Appendix*, Fig. S3). This observation suggests a systemic dysregulation of the B cell compartment as a result of ataxin-1 deficiency. In contrast, ataxin-1 ablation does not appear to affect $CD4^+$ and $CD8^+$ T cell lineages as we did not detect any significant changes in their naïve, central memory, and effector subsets, either before or after $MOG_{35–55}$ priming (*SI Appendix*, Fig. S4 *A* and *B*). The central role of B cells is further supported by the significantly higher number of B cells detected in the spinal cord parenchyma of $Atxn1^{-/-}$ mice at disease onset, while no differences were measured in infiltrating T cells (Fig. 3 *B* and *C*).

Next, we explored the role of ataxin-1 on B cell-mediated antibody production by assessing immunoglobulin levels in serum. A significant increase in total immunoglobulin M (IgM) and immunoglobulin G (IgG) was found in naïve $Atxn1^{-/-}$ mice compared to wildtype animals, and such increase in IgM levels persisted after MOG peptide immunization (*SI Appendix*, Fig. S5 *A* and *B*). We also measured the MOG peptide-specific humoral response in immunized mice and found that $Atxn1^{-/-}$ animals produce higher levels of anti-$MOG_{35–55}$ IgG antibodies while no differences were detected for anti-$MOG_{35–55}$ IgM (*SI Appendix*, Fig. S5 *C* and *D*).

Ataxin-1 Regulates B Cell Functions through Specific Genetic Programs. RNA sequencing (RNA-seq) transcriptomic profiling of B cells from naïve and MOG peptide-primed mice were performed in order to reconstruct the genetic networks controlled by ataxin-1 in response to an autoimmune challenge. Comparative analysis identified 86 differentially expressed genes (DEGs) between wildtype and knockout B cells at baseline

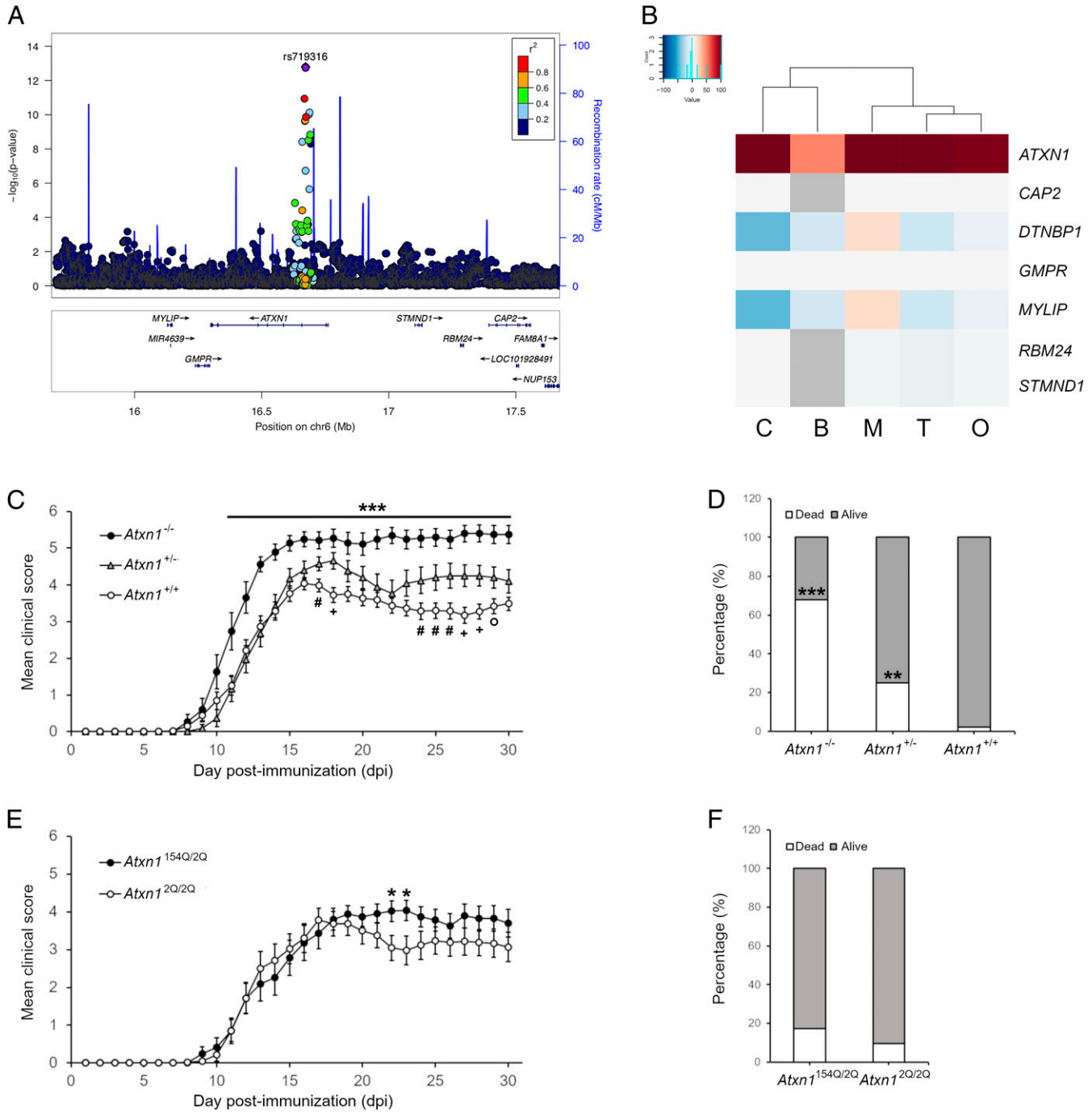

Fig. 1. Ataxin-1 exerts a protective effect on autoimmune demyelination. (*A*) The association *P* values derived from meta-analysis of all reported MS case–control studies in European ancestry populations for the SNPs at 6p22 locus are plotted. X-axis displays genomic positions based on hg19 and y-axis shows −log10 (*P* value). Top SNP (rs719316) is shown in purple and locates to the third intron of *ATXN1* gene. The other SNPs are colored by the strength of linkage disequilibrium (LD) (r^2) with the top SNP. (*B*) Analysis of the predicted regulatory effect (PRE) of rs719316 in the *ATXN1* locus. In the heatmap, each column represents a different cell type while each row represents a gene. The colors indicate positive (red), neutral (white) or negative (blue) PRE values. C = CNS, B = B cells, M = monocytes, T = T cells, O = others. (*C*) EAE induction in *Atxn1*$^{-/-}$ mice results in exacerbated disease course in comparison to controls. Heterozygous animals show instead a phenotype in between the homozygous animals (n = 19 knockout mice, n = 20 heterozygous mice, n = 38 wildtype mice). (*D*) A similar gene-dose effect is observed in mortality rates at EAE end point (30 dpi). (*E* and *F*) EAE induction in SCA1 knock-in mice (*Atxn1*$^{154Q/2Q}$) results in similar severity and mortality as compared to controls. The only exception is represented by the days 22 to 23 dpi where knock-in mice show increased scores as compared to controls (n = 23 knock-in mice, n = 21 wildtype mice). Differences between scores in each day were assessed by two-tailed Student's *t* test while differences in mortality rates were assessed by Fisher's exact test. * (knockout vs. wildtype) or (knock-in vs. wildtype); $^{\#}$, $^{+}$, and ° (heterozygous vs. wildtype). * or $^{\#}P \leq 0.05$, ** or $^{+}P \leq 0.01$, *** or ° $P \leq 0.001$.

(Fig. 4*A* and Dataset S1), while 562 DEGs were detected upon $MOG_{35–55}$ immunization (Fig. 4*B* and Dataset S1). These differences are sufficient to clearly segregate the two genotypes at both states by unsupervised hierarchical clustering. Gene ontology (GO) enrichment was performed on each DEG list to capture the biological functions associated with these genes. At

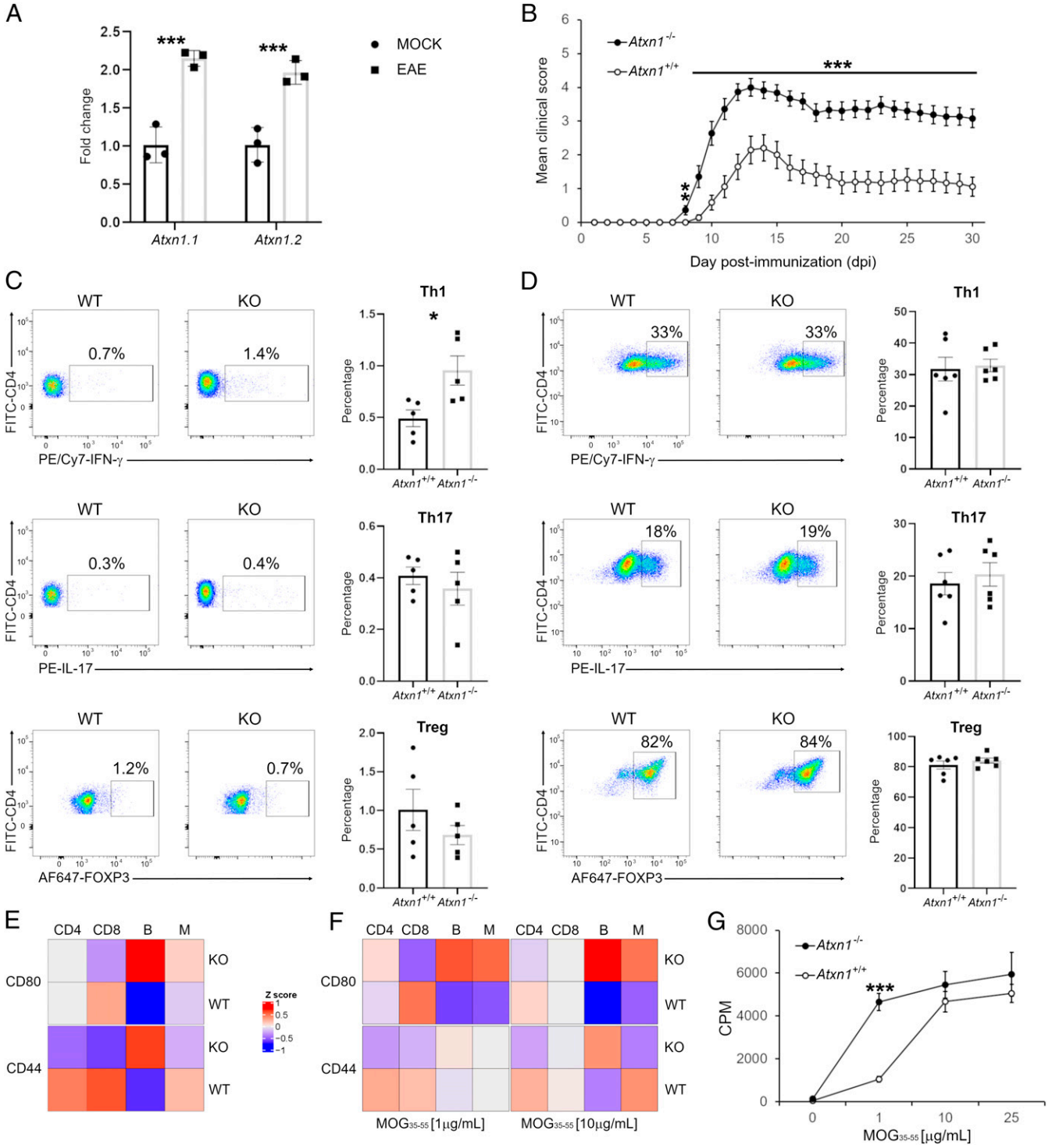

Fig. 2. Ataxin-1 regulates the immune response. (*A*) All *Atxn1* variants are up-regulated in spleens of EAE mice (20 dpi) as compared to controls ($n = 3$ mice per group). (*B*) Adoptive transfer of *Atxn1*$^{-/-}$ splenocytes drives a more severe passive EAE as compared to *Atxn1*$^{+/+}$ cells ($n = 18$ knockout mice, $n = 17$ wildtype mice). (*C*) A higher percentage of Th1 cells was measured in *Atxn1*$^{-/-}$ splenocytes from MOG peptide-primed mice restimulated in vitro ($n = 5$ mice per group). (*D*) Similar percentages of Th1, Th17, and Treg cells were measured for both genotypes in pure cultures of naïve CD4$^+$ T cells ($n = 6$ mice per group). (*E*) Surface levels of CD44 and CD80 were assessed in naïve splenocytes. In the heatmap, each column represents the mean of all mice in the group for each cytotype and each row the levels of a specific marker. The levels of both markers are increased in knockout B cells ($P_{CD44} = 0.003$; $P_{CD80} = 0.0006$) while CD44 is more expressed in wildtype CD4$^+$ ($P = 0.05$) and CD8$^+$ ($P = 0.009$) cells ($n = 11$ mice per group). (*F*) CD44 and CD80 surface levels were measured in splenocytes from MOG peptide-primed mice and restimulated in vitro. Higher levels of CD80 were detected in knockout B cells ($P_{MOG1} = 0.01$; $P_{MOG10} = 0.002$) and monocytes ($P_{MOG1} = 0.03$; $P_{MOG10} = 0.05$) ($n = 8$ mice per group). (*G*) Naïve CD4$^+$ T cells from 2D2 mice were cocultured with B cells in the presence of increasing concentrations of MOG peptide. Knockout B cells showed increased antigen presenting activity as demonstrated by higher T cell proliferation rates ($n = 3$ mice per group). Differences between groups were assessed by two-tailed Student's *t* test. $^*P \leq 0.05$, $^{**}P \leq 0.01$, $^{***}P \leq 0.001$.

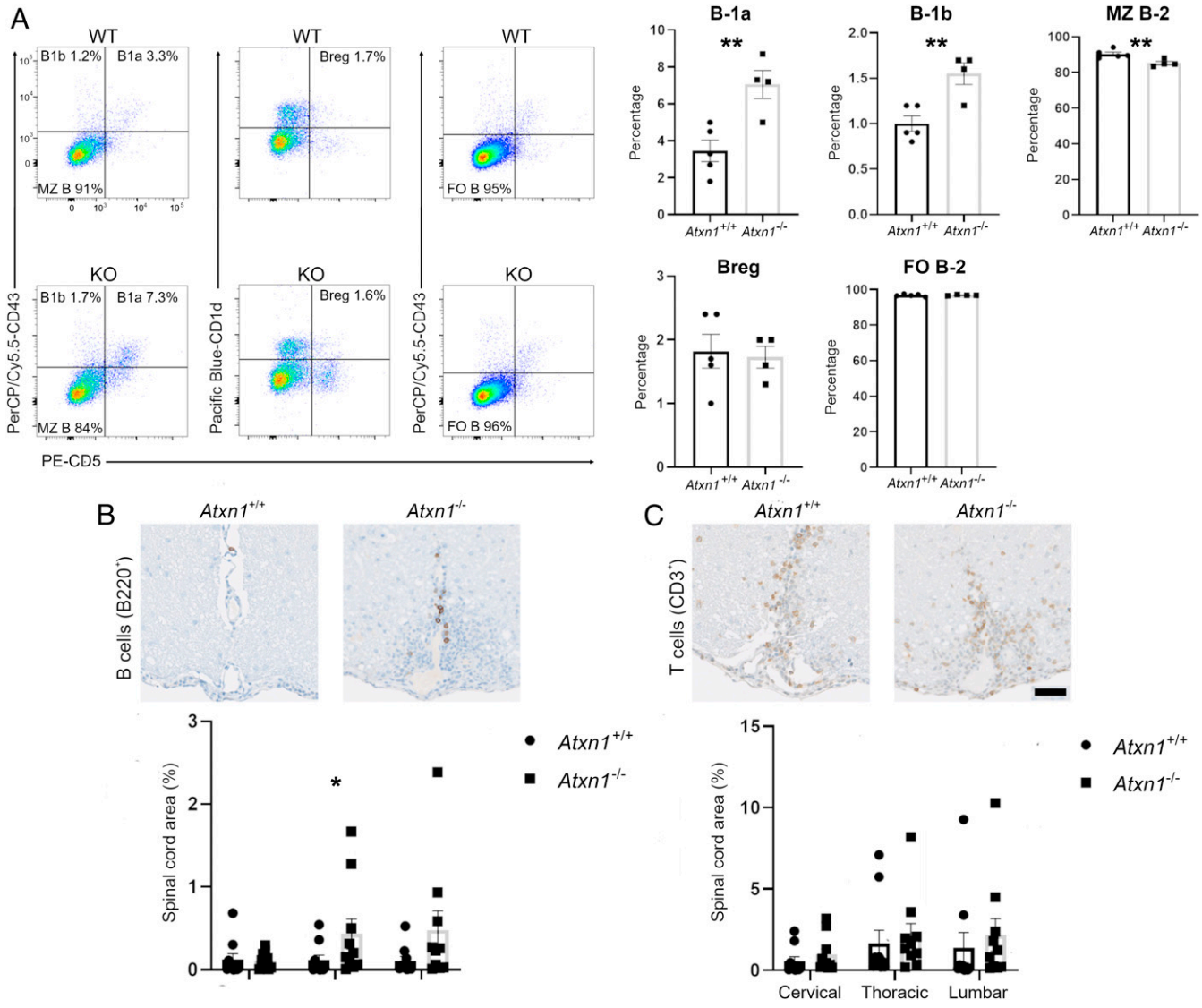

Fig. 3. Ataxin-1 controls the functions of the B cell compartment. (*A*) Splenocytes from *Atxn1*$^{-/-}$ and wildtype mice were analyzed by flow cytometry for different CD19^{+} B cell subpopulations. A significant increase was measured for the percentage of B-1a [CD5^{+},CD43^{+},IgM^{high}, immunoglobulin D (IgD)^{low}] and B-1b (CD5^{-},CD43^{+},IgM^{high},IgD^{low}) subsets in knockout animals as compared to controls, while marginal zone B-2 cells (CD5^{-},CD43^{-},IgM^{high},IgD^{low}) were significantly decreased. No differences were instead measured in the size of regulatory (CD5^{+},CD43^{-},IgM^{high},IgD^{low}) and follicular B-2 (CD5^{-},CD43^{-},IgM^{low},IgD^{high}) cell populations between the two genotypes (n = 4 to 5 mice per group). (*B*) Histological analysis of B cell infiltration into the spinal cord of *Atxn1*$^{-/-}$ and wildtype mice upon EAE. Paraffin-embedded sections from spinal cords (cervical, thoracic, and lumbar regions) were collected at EAE onset (10 dpi) and stained for B cells using an antibody for B220. Digital images were then acquired and B cell infiltration was measured as the area positive to B220 stain relative to the total area of the spinal cord section. A significant increase in infiltrating B cells was quantified in the thoracic region of *Atxn1*$^{-/-}$ mice (n = 10 mice per group). (*C*) T cell infiltration was similarly assessed using an antibody for CD3. No significant differences were detected between genotypes (n = 10 mice per group). Scale bar: 50 μm. Differences in the size of cell populations were assessed by two-tailed Student's t test while differences in cell infiltration were assessed by one-tailed Student's t test. *$P \leq 0.05$, **$P \leq 0.01$.

baseline, "regulation of cell activation" (fold increase: 5.4, $P_{corr} = 10^{-7}$) resulted in the top GO term (Fig. 4*C* and Dataset S2), while "mitotic cell cycle progress" (fold increase: 4.7, $P_{corr} = 10^{-26}$) was the most significant ontology in primed cells (Fig. 4*D* and Dataset S2). Independent validation by qRT-PCR amplification of 33 candidate genes confirmed the RNA-seq results (*SI Appendix*, Tables S2 and S3). Network analysis also highlighted that $MOG_{35–55}$ responsive genes are enriched in protein-protein interactions ($P < 10^{-16}$) as components of the mitotic molecular machinery (Fig. 4*E*). Conversely, no enrichment in physical interactions was found for baseline DEGs. Ataxin-1 inhibits the expression of target genes through its binding partner CIC, for which specific binding motifs are known (21). Consequently, we screened the promoter regions of all of the DEGs for the presence of two known CIC-binding motifs, TGAATGAA and TGAATGGA, and observed a significant enrichment only for the former at baseline (fold increase: 2.6, $P = 0.03$). From these results, we conclude that baseline DEGs are likely to be direct targets of ataxin-1 while the transcriptional changes taking place after $MOG_{35–55}$ stimulation represent secondary events.

Longitudinal comparisons were also performed within each genotype to identify those genes dynamically regulated along the immune response. By comparing the transcriptomic profiles at baseline and upon MOG peptide immunization, 210 DEGs were found in wildtype cells and 867 DEGs in knockout cells (*SI Appendix*, Fig. S6 *A* and *B* and Dataset S1), with an overlap of

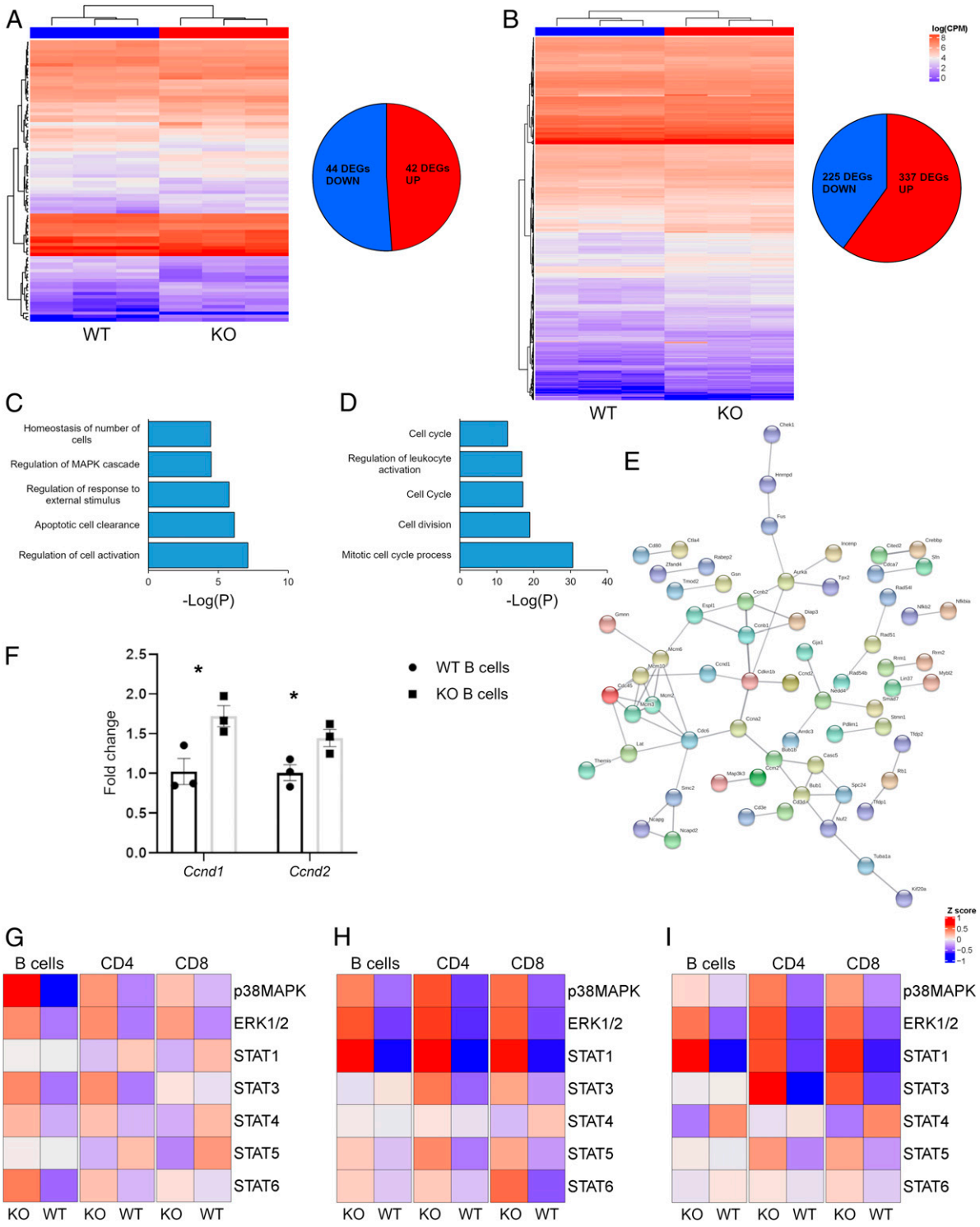

Fig. 4. Ataxin-1 controls B cell proliferation. (*A* and *B*) Unsupervised clustering of the DEGs separates *Atxn1*$^{-/-}$ and wildtype B cells at baseline and 10 dpi (n = 3 per group). (*C* and *D*) Histograms showing the top five most significant GO terms at baseline and 10 dpi, respectively. (*E*) Protein network built using the DEGs from the primed B cells as input. (*F*) Validation of *Ccnd1* and *Ccnd2* expression by qRT-PCR (n = 3 mice per group). (*G*) The activation status of seven phosphoproteins was assessed in naïve splenocytes (n = 11 mice per group). p38MAPK was hyperphosphorylated in *Atxn1*$^{-/-}$ B cells as compared to wildtype cells ($P = 0.008$). (*H*) The same phosphoproteins were also tested in splenocytes at 10 dpi (n = 8 mice per group). ERK1/2 was hyperphosphorylated in all of the tested knockout cytotypes ($P_{CD4} = 0.002$; $P_{CD8} = 0.01$; $P_{B\ cells} = 0.007$). The same trend was observed for STAT1 ($P_{CD4} = 0.0002$; $P_{CD8} = 0.0004$; $P_{B\ cells} = 0.0003$), while p38MAPK was hyperphosphorylated only in knockout T cells ($P_{CD4} = 0.01$; $P_{CD8} = 0.03$). STAT3 was hyperphosphorylated only in knockout CD4$^+$ cells (P = 0.04) and STAT6 only in knockout CD8$^+$ cells ($P = 0.02$). (*I*) The same seven phosphoproteins were analyzed in primed splenocytes restimulated in vitro (n = 8 mice per group). STAT1 was hyperphosphorylated in both knockout T and B cells ($P_{CD4} = 0.02$; $P_{CD8} = 0.008$; $P_{B\ cells} = 0.004$) while STAT3 was more activated in knockout T cells ($P_{CD4} = 0.003$; $P_{CD8} = 0.03$). ERK1/2 phosphorylation was increased in knockout CD4$^+$ cells ($P = 0.02$). In the heatmaps, each column represents the mean of all mice in the group for each cytotype and each row the levels of a specific phosphoprotein. Differences between groups were assessed by two-tailed Student's t test $^*P \leq 0.05$, $^{**}P \leq 0.01$, $^{***}P \leq 0.001$.

107 genes (*SI Appendix*, Fig. S6*C*). GO analysis on the knockout B cell-specific 760 DEGs identified the term "inflammation response" as the most significantly enriched (fold increase: 3.0, $P_{corr} = 10^{-11}$) (*SI Appendix*, Fig. S6*D* and Dataset S2). Independent qRT-PCR validation on 17 genes contributing to this ontology confirmed their up-regulation in MOG peptide-stimulated knockout B cells, including the interleukin-18 (IL-18) encoding *Il18* and the complement components *C1qa*, *C1qb*, *C1qc*, and *C6* (*SI Appendix*, Table S4). No differences were measured in the expression of the same genes in wildtype B cells (*SI Appendix*, Table S5). Longitudinal analysis also highlighted the significant up-regulation of genes encoding matrix metalloproteinases (*Mmp8*, *Mmp9*, *Mmp11*, *Mmp13*, *Mmp14*, *Mmp25*, *Mmp27*) in knockout B cells upon MOG peptide stimulation (*SI Appendix*, Fig. S7*A*). No differences were instead found for the *Mmp* genes expressed in wildtype B cells (*SI Appendix*, Fig. S7*B*). This is consistent with the higher B cell infiltration observed in the spinal cord of *Atxn1*$^{-/-}$ mice, and with previous reports implicating the ATXN1 protein family in extracellular matrix remodeling (7).

MAPK and STAT Signaling Pathways Are Modulated by Ataxin-1 in B Cells. Collectively, our analysis highlights a repressing activity for ataxin-1 on B cell activation, cytokine production, and proliferation. In fact, key factors for G-to-S phase transition such as cyclins D1 and D2 (*Ccnd1* and *Ccnd2*) were overexpressed in knockout cells as confirmed by quantitative RT-PCR (Fig. 4*F*). A link between ataxin-1 and cell proliferation has been recently described, and mitogen-activated protein kinase (MAPK) signaling was shown to be critical in mediating this function (22). The "regulation of MAPK cascade" term was found enriched also in our GO analysis, supporting its possible involvement in B cell proliferation. We sought to experimentally test this hypothesis by employing phosphoflow cytometry to profile the activation status of the main intracellular pathways in different immune cell populations before and after MOG stimulation. Multiple cascades were hyperactivated in knockout cells. Among them, the MAPK pathways p38 and extracellular signal-regulated kinase (ERK)1/2 showed higher phosphorylation levels in knockout B cells respectively at baseline (Fig. 4*G* and *SI Appendix*, Table S6) and after MOG peptide stimulation (Fig. 4*H* and *SI Appendix*, Table S7). Furthermore, several signal transducer and activator of transcription (STAT) cascades were found hyperphosphorylated in both knockout T and B cells after MOG peptide priming, and their activation persisted also upon MOG peptide restimulation in vitro (Fig. 4*I* and *SI Appendix*, Table S8). Notably, STAT1 activation in $CD4^+$ T cells is required for optimal Th1 development (23).

The ATXN1-CIC Axis Is Critical for B Cell-Dependent Immunomodulation. From a molecular standpoint, ataxin-1 works in concert with its paralog ataxin-1 like (ATXN1L) protein to bind and stabilize CIC (7, 24). Notably, *Cic* is significantly down-regulated in B cells upon MOG peptide stimulation while no differences were detected in the levels of *Atxn1* and *Atxn1l* transcripts (*SI Appendix*, Fig. S8). To confirm in vivo the role of ataxin-1 in B cells and assess whether its immunomodulatory activity is mediated by the same set of native interactions, we generated a panel of conditional knockout lines to selectively disrupt the ATXN1-ATXN1L-CIC complex in relevant immune cell lineages. Specifically, we bred transgenic mice in which *Atxn1l* or *Cic* gene has been floxed (5) with *Cd19-Cre* or *Cd79a-Cre* drivers for B cell-targeted knockout (25, 26). As a control, we also crossed them with a driver line in which the Cre-recombinase is under the control of the human *CD2* promoter, for efficient deletion in both $CD4^+$ and $CD8^+$ T cells (27). We then induced EAE in each conditional knockout line and followed disease course up to 30 dpi. We found that mice lacking CIC in B cells display a significantly more severe disease at peak (15 to 16 dpi) than floxed controls (Fig. 5*A*), while no differences were measured in mice lacking ATXN1L in B cells (Fig. 5*B*). This is likely due to insufficient CIC destabilization as a consequence of ATXN1L ablation (*SI Appendix*, Fig. S9 *A* and *B*). Also, as suggested by our in vitro experiments on isolated $CD4^+$ T cells, knocking out neither *Cic* nor *Atxn1l* in T lymphocytes influenced the EAE course (Fig. 5 *C* and *D*).

Discussion

Here, we present the functional characterization of the MS risk locus mapping to chromosome 6p22 in which the strongest association was detected in the ataxin-1 encoding *ATXN1* gene. Specifically, ataxin-1 controls distinct genetic programs that limit excessive proliferation and activation of B cells in a proinflammatory milieu. The lack of ataxin-1 regulatory activity results in an exaggerated immune activation that eventually leads to a Th1/Th2 ratio imbalance, amplifying the autoimmune injury. The current working hypothesis for MS pathogenesis postulates that aberrant immune responses are driven by the transcriptional dysregulation of a specific set of genes (11, 28, 29). The present findings further support this paradigm whereby ataxin-1 represents a high-rank repressor of gene expression for multiple genes and biochemical pathways. Several studies aimed at identifying the genetic targets of ataxin-1. For instance, microarray profiling of cerebellar tissues from *Atxn1*-null mice identified alterations in the expression of genes regulated by Sp1-dependent transcription, such as dopamine receptor D2 (*Drd2*) and retinoic acid/thyroid hormone (30). Gene expression analysis in the cerebellum of the knock-in SCA1 model highlighted alterations in the insulin-like growth factor pathway (31), and the use of laser-capture to isolate Purkinje neurons from knock-in mouse cerebella led to the identification of the vascular endothelial growth factor (*Vegf*) as a direct target of ataxin-1 (32). Our transcriptional profiling of *Atxn1*$^{-/-}$ B cells showed that numerous components of the mitotic apparatus including the cyclins D1 and D2 are up-regulated in response to MOG peptide stimulation. This correlates with the expansion of specific B cell subsets that can modulate EAE pathology such as B-1a cells (33). B-1 cells have been also found increased in the cerebrospinal fluid of MS patients and CD5 expression on their surface correlates with disease activity (34, 35). Interestingly, increased levels of cyclin D1 were also reported in the cerebellum of SCA1 knock-in mice (36), pointing at cell cycle dysregulation of specific cell niches as an underlying mechanism in both neurodegeneration and autoimmunity. Consistent with this model, the pathological expansion of cerebellar stem cells has been recently found in postnatal SCA1 mice (37). Transcriptomic analysis also revealed that specific genes encoding proinflammatory factors are selectively up-regulated in *Atxn1*$^{-/-}$ B cells upon MOG peptide stimulation. Noteworthy, among them, the IL-18 cytokine promotes Th1 activity and self-reactive IgG and IgM antibody responses (38, 39), which is consistent with our observations of increased Th1 lymphocytes and antibody titers in *Atxn1*$^{-/-}$ mice. Genes encoding complement proteins were also up-regulated in primed knockout B cells. This cascade modulates EAE progression and is required for development of maximal disease (40). Complement genes are also associated with neurodegenerative phenotypes in MS (41).

In addition to exaggerated cell proliferation, we found an increased humoral response as a consequence of ataxin-1 deficiency in B cells. Autoantibodies against murine recombinant MOG and MOG peptide are not generally considered pathogenic due to a proline to serine substitution at position 42 between murine and human proteins (42). However, a small body of experimental evidence exists, suggesting the potential involvement of antibodies anti-murine MOG peptide in modulating disease. Serum levels of anti-$MOG_{35–55}$ IgGs correlate with disease progression (43), and passive transfer of serum from MOG peptide immunized mice was shown to aggravate EAE severity in wildtype mice (44). Moreover, anti-$MOG_{35–55}$ antibodies were confirmed to target neural

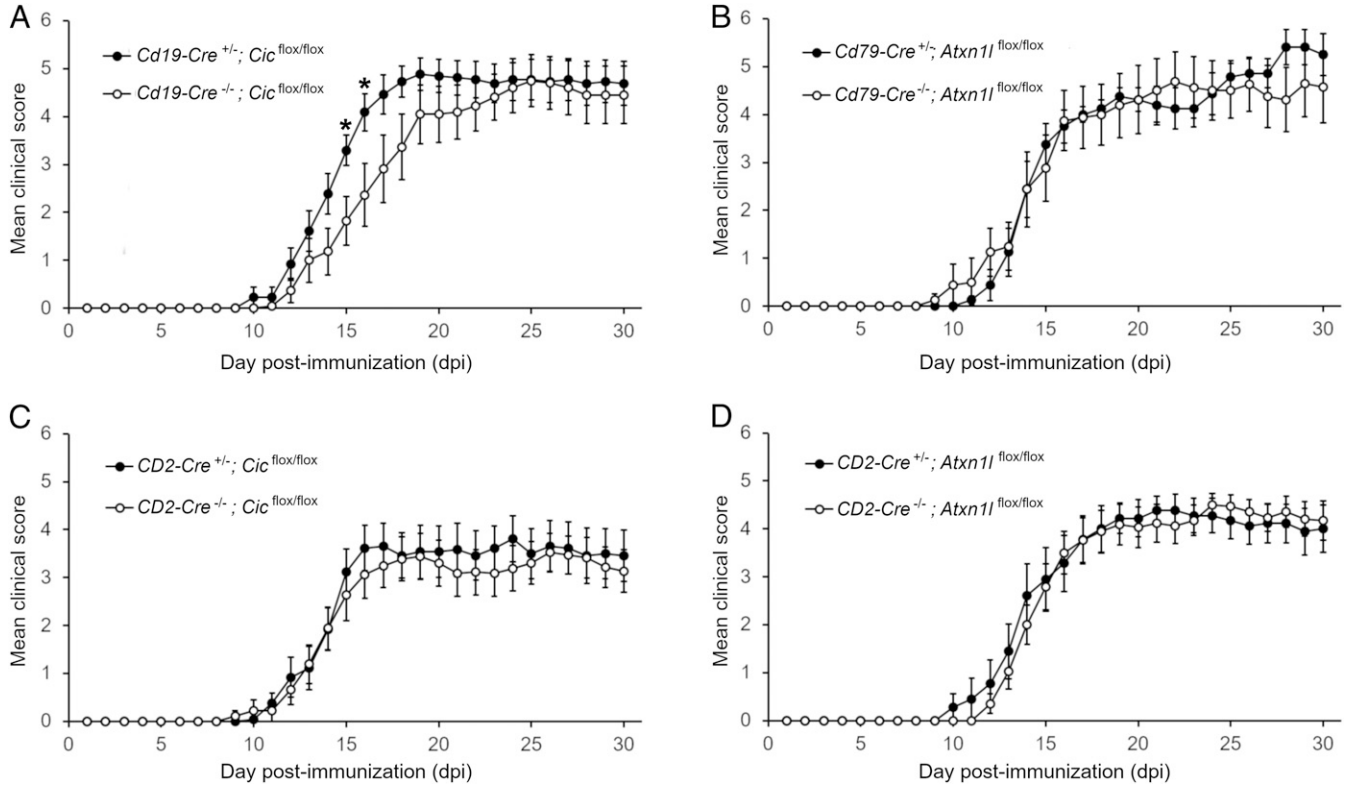

Fig. 5. Ataxin-1 mediates its immunoregulatory function in B cells through CIC interactions. (*A* and *B*) EAE was induced in conditional knockout lines in which the ataxin-1 interactors CIC and ATXN1L were selectively ablated in the B cell lineage using B cell-specific Cre drivers (*Cd19-Cre* or *Cd79-Cre*). B cell-specific CIC-null mice showed more severe disease at peak (15 to 16 dpi) as compared to floxed littermates ($Cre^{-/-}$), while no statistically significant differences were detected in the EAE course of B cell-specific ATXN1L-null animals and controls (n = 18 $Cd19\text{-}Cre^{+/-}$;$Cic^{flox/flox}$ mice, n = 12 $Cd19\text{-}Cre^{-/-}$;$Cic^{flox/flox}$ mice, n = 8 $Cd79\text{-}Cre^{+/-}$;$Atxn1l^{flox/flox}$ mice, n = 8 $Cd79\text{-}Cre^{-/-}$;$Atxn1l^{flox/flox}$ mice). (*C* and *D*) Conditional knockout lines in which CIC and ATXN1L were selectively ablated in T cells were also generated using a *CD2-Cre* driver. No differences in the EAE phenotype were measured in both lines as compared to their floxed littermates (n = 18 $CD2\text{-}Cre^{+/-}$;$Cic^{flox/flox}$ mice, n = 13 $CD2\text{-}Cre^{-/-}$;$Cic^{flox/flox}$ mice, n = 9 $CD2\text{-}Cre^{+/-}$;$Atxn1l^{flox/flox}$ mice, n = 17 $CD2\text{-}Cre^{-/-}$;$Atxn1l^{flox/flox}$ mice). Differences between scores in each day were assessed by two-tailed Student's t test $^*P \leq 0.05$.

precursor cells (NPCs) in the subventricular zone of the hippocampus and trigger apoptotic pathways (45).

Another relevant finding of the present study is the central role that ATXN1-CIC interactions play in mediating the immunomodulatory effects on B cells. CIC is a transcriptional repressor of the high mobility group (HMG)-box family, which binds specific DNA sites in target genes. Beyond its role in SCA1 and neurodevelopment, CIC's repressing activity was shown to exert tumor suppressive functions, and damaging mutations in the *CIC* gene have been associated with the development and progression of several neoplastic syndromes (46). Intriguingly, CIC loss-of-function was also demonstrated to promote aberrant activation of adaptive immunity via excessive development of follicular helper T cells and germinal center (GC) responses (47). Our data add to this picture a suppressive function for CIC also on exaggerated activation and proliferation of B cells in response to encephalitogenic challenges. At the molecular level, CIC is a downstream effector of the ERK pathway and its binding to target genes is abolished by phosphorylation at conserved serine residues (48), either due to decreased protein stability or increased cytoplasmic translocation. The phosphoflow analysis conducted here found this cascade significantly hyperactivated in $Atxn1^{-/-}$ B cells. Hence, we argue that cell cycle dysregulation in knockout B cells presumably takes place via ERK-dependent CIC inactivation. It is interesting that ablation of the other ataxin-1 interactor ATXN1L failed to recapitulate the effects on EAE phenotype of ataxin-1 or CIC depletion. These results indicate that CIC is the likely downstream effector of ataxin-1 activity while ATXN1L's presence in the complex is dispensable, probably due to its redundancy with ataxin-1. In fact, we did not observe a reduction in CIC levels upon ATXN1L ablation in B cells. This is in line with previous reports showing that *Atxn1l* knockout mice could only partially phenocopy double *Atxn1-Atxn1l* animals (7).

Lastly, these results further support the pathogenic role for B cells in starting CNS autoimmunity linked, at least in part, to the individual genetic signature. The interest in B cells in MS pathogenesis has been recently fueled by successful therapeutic depleting strategies (49). In EAE, B cells can exert opposite effects, either pathogenic or protective, depending on the specific encephalitogen adopted for immunization and reflecting the engagement of distinct B cell subsets and mechanisms of action (50). In the $MOG_{35–55}$ paradigm, B cell depletion was demonstrated to worsen the disease due to the removal of interleukin 10 (IL-10) producing regulatory B cells (51). Some authors have also reported that B cell depletion after immunization ameliorates the phenotype through ablation of interleukin 6 (IL-6) producing pathogenic B cells (52). EAE is an imperfect model for MS and a number of caveats should be considered when translating evidence collected in this animal disease to the human counterpart. Although the contribution of ataxin-1-mediated mechanisms taking place in CNS cells cannot be ruled out, the data highlight a previously unrecognized role of ataxin-1 in B cell biology and neuroinflammation, and suggests the ataxin-1-CIC pathway as a possible checkpoint to target autoimmune demyelination.

Materials and Methods

All animal procedures were performed in compliance with experimental guidelines approved by the University of California, San Francisco Committee on Animal Research (CAR). Details on the different mouse lines employed in this study as well as on the protocols for inducing EAE and for histopathological analyses are provided in the *SI Appendix*. Details on antibodies, Western blotting, cell activation and differentiation assays, T-B cell cocultures, phosphoflow cytometry, immunophenotyping, immunoglobulin quantification, RNA-seq, quantitative RT-PCR, bioinformatic and statistical analyses are also provided in the *SI Appendix*.

Data Availability. All study data are included in the article and *SI Appendix*.

ACKNOWLEDGMENTS. The authors thank Dr. Huda Zoghbi (Baylor College of Medicine, Houston, TX) for the kind gift of the conditional mouse lines. The authors acknowledge the contributions of Dr. Nikolaos A. Patsopoulos and Dr. Sergio E. Baranzini to the statistical and bioinformatics analysis of the human genome wide association study dataset. This study was supported by a grant from the US National Multiple Sclerosis Society (RG-1901-33219) and NIH (RO1NS26799). The study was also supported by FISM-Fondazione Italiana Sclerosi Multipla Senior Research Fellowships Cod.2014/B/1 and Cod. 2017/B/3, and financed or cofinanced with the "5 per mille" public funding.

1. H. T. Orr *et al*., Expansion of an unstable trinucleotide CAG repeat in spinocerebellar ataxia type 1. *Nat. Genet.* **4**, 221–226 (1993).
2. H. Y. Zoghbi, H. T. Orr, Pathogenic mechanisms of a polyglutamine-mediated neurodegenerative disease, spinocerebellar ataxia type 1. *J. Biol. Chem.* **284**, 7425–7429 (2009).
3. Y. C. Lam *et al*., ATAXIN-1 interacts with the repressor Capicua in its native complex to cause SCA1 neuropathology. *Cell* **127**, 1335–1347 (2006).
4. A. Matilla *et al*., Mice lacking ataxin-1 display learning deficits and decreased hippocampal paired-pulse facilitation. *J. Neurosci.* **18**, 5508–5516 (1998).
5. H. C. Lu *et al*., Disruption of the ATXN1-CIC complex causes a spectrum of neurobehavioral phenotypes in mice and humans. *Nat. Genet.* **49**, 527–536 (2017).
6. M. Asher, A. Johnson, B. Zecevic, D. Pease, M. Cvetanovic, Ataxin-1 regulates proliferation of hippocampal neural precursors. *Neuroscience* **322**, 54–65 (2016).
7. Y. Lee *et al*., ATXN1 protein family and CIC regulate extracellular matrix remodeling and lung alveolarization. *Dev. Cell* **21**, 746–757 (2011).
8. A. R. Kang, H. T. An, J. Ko, S. Kang, Ataxin-1 regulates epithelial-mesenchymal transition of cervical cancer cells. *Oncotarget* **8**, 18248–18259 (2017).
9. J. Suh *et al*., Loss of ataxin-1 potentiates Alzheimer's pathogenesis by elevating cerebral BACE1 transcription. *Cell* **178**, 1159–1175.e17 (2019).
10. S. L. Hauser, J. R. Oksenberg, The neurobiology of multiple sclerosis: Genes, inflammation, and neurodegeneration. *Neuron* **52**, 61–76 (2006).
11. International Multiple Sclerosis Genetics Consortium, Multiple sclerosis genomic map implicates peripheral immune cells and microglia in susceptibility. *Science* **365**, eaav7188 (2019).
12. N. Isobe *et al*.; International Multiple Sclerosis Genetics Consortium, An ImmunoChip study of multiple sclerosis risk in African Americans. *Brain* **138**, 1518–1530 (2015).
13. International Multiple Sclerosis Genetics Consortium, A systems biology approach uncovers cell-specific gene regulatory effects of genetic associations in multiple sclerosis. *Nat. Commun.* **10**, 2236 (2019).
14. S. S. Zamvil, L. Steinman, Diverse targets for intervention during inflammatory and neurodegenerative phases of multiple sclerosis. *Neuron* **38**, 685–688 (2003).
15. P. J. Thul *et al*., A subcellular map of the human proteome. *Science* **356**, eaal3321 (2017).
16. V. K. Kuchroo *et al*., B7-1 and B7-2 costimulatory molecules activate differentially the Th1/Th2 developmental pathways: Application to autoimmune disease therapy. *Cell* **80**, 707–718 (1995).
17. H. Guan, P. S. Nagarkatti, M. Nagarkatti, Role of CD44 in the differentiation of Th1 and Th2 cells: CD44-deficiency enhances the development of Th2 effectors in response to sheep RBC and chicken ovalbumin. *J. Immunol.* **183**, 172–180 (2009).
18. C. R. Parker Harp *et al*., B cell antigen presentation is sufficient to drive neuroinflammation in an animal model of multiple sclerosis. *J. Immunol.* **194**, 5077–5084 (2015).
19. E. R. Pierson, I. M. Stromnes, J. M. Goverman, B cells promote induction of experimental autoimmune encephalomyelitis by facilitating reactivation of T cells in the central nervous system. *J. Immunol.* **192**, 929–939 (2014).
20. N. Baumgarth, The double life of a B-1 cell: Self-reactivity selects for protective effector functions. *Nat. Rev. Immunol.* **11**, 34–46 (2011).
21. M. Kawamura-Saito *et al*., Fusion between CIC and DUX4 up-regulates PEA3 family genes in Ewing-like sarcomas with t(4;19)(q35;q13) translocation. *Hum. Mol. Genet.* **15**, 2125–2137 (2006).
22. A. R. Kang, H. T. An, J. Ko, E. J. Choi, S. Kang, Ataxin-1 is involved in tumorigenesis of cervical cancer cells via the EGFR-RAS-MAPK signaling pathway. *Oncotarget* **8**, 94606–94618 (2017).
23. A. Takeda *et al*., Cutting edge: Role of IL-27/WSX-1 signaling for induction of T-bet through activation of STAT1 during initial Th1 commitment. *J. Immunol.* **170**, 4886–4890 (2003).
24. E. Kim, H. C. Lu, H. Y. Zoghbi, J. J. Song, Structural basis of protein complex formation and reconfiguration by polyglutamine disease protein Ataxin-1 and Capicua. *Genes Dev.* **27**, 590–595 (2013).
25. E. Hobeika *et al*., Testing gene function early in the B cell lineage in mb1-cre mice. *Proc. Natl. Acad. Sci. U.S.A.* **103**, 13789–13794 (2006).
26. R. C. Rickert, J. Roes, K. Rajewsky, B lymphocyte-specific, Cre-mediated mutagenesis in mice. *Nucleic Acids Res.* **25**, 1317–1318 (1997).
27. M. S. Vacchio *et al*., A ThPOK-LRF transcriptional node maintains the integrity and effector potential of post-thymic CD4+ T cells. *Nat. Immunol.* **15**, 947–956 (2014).
28. International Multiple Sclerosis Genetics Consortium, Low-frequency and rare-coding variation contributes to multiple sclerosis risk. *Cell* **175**, 1679–1687.e7 (2018).
29. M. Ban *et al*., Transcript specific regulation of expression influences susceptibility to multiple sclerosis. *Eur. J. Hum. Genet.* **28**, 826–834 (2020).
30. R. Goold *et al*., Down-regulation of the dopamine receptor D2 in mice lacking ataxin 1. *Hum. Mol. Genet.* **16**, 2122–2134 (2007).
31. J. R. Gatchel *et al*., The insulin-like growth factor pathway is altered in spinocerebellar ataxia type 1 and type 7. *Proc. Natl. Acad. Sci. U.S.A.* **105**, 1291–1296 (2008).
32. M. Cvetanovic, J. M. Patel, H. H. Marti, A. R. Kini, P. Opal, Vascular endothelial growth factor ameliorates the ataxic phenotype in a mouse model of spinocerebellar ataxia type 1. *Nat. Med.* **17**, 1445–1447 (2011).
33. L. K. Peterson, I. Tsunoda, R. S. Fujinami, Role of CD5+ B-1 cells in EAE pathogenesis. *Autoimmunity* **41**, 353–362 (2008).
34. E. Mix *et al*., B cells expressing CD5 are increased in cerebrospinal fluid of patients with multiple sclerosis. *Clin. Exp. Immunol.* **79**, 21–27 (1990).
35. O. A. Seidi, Y. K. Semra, M. K. Sharief, Expression of CD5 on B lymphocytes correlates with disease activity in patients with multiple sclerosis. *J. Neuroimmunol.* **133**, 205–210 (2002).
36. J. Crespo-Barreto, J. D. Fryer, C. A. Shaw, H. T. Orr, H. Y. Zoghbi, Partial loss of ataxin-1 function contributes to transcriptional dysregulation in spinocerebellar ataxia type 1 pathogenesis. *PLoS Genet.* **6**, e1001021 (2010).
37. C. R. Edamakanti, J. Do, A. Didonna, M. Martina, P. Opal, Mutant ataxin1 disrupts cerebellar development in spinocerebellar ataxia type 1. *J. Clin. Invest.* **128**, 2252–2265 (2018).
38. F. D. Shi, K. Takeda, S. Akira, N. Sarvetnick, H. G. Ljunggren, IL-18 directs autoreactive T cells and promotes autodestruction in the central nervous system via induction of IFN-gamma by NK cells. *J. Immunol.* **165**, 3099–3104 (2000).
39. S. L. Enoksson *et al*., The inflammatory cytokine IL-18 induces self-reactive innate antibody responses regulated by natural killer T cells. *Proc. Natl. Acad. Sci. U.S.A.* **108**, E1399–E1407 (2011).
40. A. J. Szalai, X. Hu, J. E. Adams, S. R. Barnum, Complement in experimental autoimmune encephalomyelitis revisited: C3 is required for development of maximal disease. *Mol. Immunol.* **44**, 3132–3136 (2007).
41. K. C. Fitzgerald *et al*., Early complement genes are associated with visual system degeneration in multiple sclerosis. *Brain* **142**, 2722–2736 (2019).
42. C. B. Marta, A. R. Oliver, R. A. Sweet, S. E. Pfeiffer, N. H. Ruddle, Pathogenic myelin oligodendrocyte glycoprotein antibodies recognize glycosylated epitopes and perturb oligodendrocyte physiology. *Proc. Natl. Acad. Sci. U.S.A.* **102**, 13992–13997 (2005).
43. P. H. Lalive, N. Molnarfi, M. Benkhoucha, M. S. Weber, M. L. Santiago-Raber, Antibody response in MOG(35-55) induced EAE. *J. Neuroimmunol.* **240-241**, 28–33 (2011).
44. C. Du, S. Sriram, Increased severity of experimental allergic encephalomyelitis in lyn-/- mice in the absence of elevated proinflammatory cytokine response in the central nervous system. *J. Immunol.* **168**, 3105–3112 (2002).
45. E. Kesidou *et al*., Humoral response in experimental autoimmune encephalomyelitis targets neural precursor cells in the central nervous system of naive rodents. *J. Neuroinflammation* **14**, 227 (2017).
46. L. Simón-Carrasco, G. Jiménez, M. Barbacid, M. Drosten, The capicua tumor suppressor: A gatekeeper of Ras signaling in development and cancer. *Cell Cycle* **17**, 702–711 (2018).
47. S. Park *et al*., Capicua deficiency induces autoimmunity and promotes follicular helper T cell differentiation via derepression of ETV5. *Nat. Commun.* **8**, 16037 (2017).
48. K. Dissanayake *et al*., ERK/p90(RSK)/14-3-3 signalling has an impact on expression of PEA3 Ets transcription factors via the transcriptional repressor capicúa. *Biochem. J.* **433**, 515–525 (2011).
49. S. L. Hauser, S. Belachew, L. Kappos, Ocrelizumab in primary progressive and relapsing multiple sclerosis. *N. Engl. J. Med.* **376**, 1694 (2017).
50. N. Molnarfi *et al*., MHC class II-dependent B cell APC function is required for induction of CNS autoimmunity independent of myelin-specific antibodies. *J. Exp. Med.* **210**, 2921–2937 (2013).
51. M. S. Weber *et al*., B-cell activation influences T-cell polarization and outcome of anti-CD20 B-cell depletion in central nervous system autoimmunity. *Ann. Neurol.* **68**, 369–383 (2010).
52. T. A. Barr *et al*., B cell depletion therapy ameliorates autoimmune disease through ablation of IL-6-producing B cells. *J. Exp. Med.* **209**, 1001–1010 (2012).